The Astronomical Journal, 139:630–635, 2010 February doi:10.1088/0004-6256/139/2/630

LUMINOUS STAR-FORMING GALAXIES IN THE *GALAXY EVOLUTION EXPLORER*–SLOAN DIGITAL SKY SURVEY DATABASE

J. B. Hutchings[1] and L. Bianchi[2]
[1] Herzberg Institute of Astrophysics, 5071 West Saanich Rd., Victoria, BC, V9E 2E7, Canada
[2] Department of Physics and Astronomy, Johns Hopkins University, 3400 N. Charles St., Baltimore, MD 21218, USA
Received 2009 August 28; accepted 2009 December 8; published 2010 January 12

ABSTRACT

We have a *Galaxy Evolution Explorer*–Sloan Digital Sky Survey sample that isolates intermediate redshift QSOs. Some 1% of the spectroscopic sample consists of galaxies in starburst or post-starburst stages. We discuss the most luminous 10 of these, which have redshifts between 0.18 and 0.6. We present spectroscopic measures and derive star formation rates. Two of the six with Mg II coverage reveal outflows in this line. None shows any sign of active galactic nucleus activity. We discuss their star formation histories and their place in galaxy evolution.

Key words: galaxies: evolution – galaxies: starburst

1. INTRODUCTION AND DATA

We are studying a sample of ∼50,000 QSO candidates selected by combined Sloan Digital Sky Survey (SDSS) and *Galaxy Evolution Explorer* (*GALEX*) photometry, for objects with strong Lyman discontinuities in the redshift range 0.5–2.0. Bianchi et al. (2009) and Bianchi (2009, and references therein) describe the sample selection considerations. SDSS spectra exist for a subset of ∼4500 objects. Among these, there are 85 spectra classified as galaxies in the SDSS database. We have examined these spectra and find that about half are QSOs. The remaining spectra are of galaxies, mostly with active star formation or young stellar populations. The most luminous of these are remarkable for their total luminosity and stellar populations, and we discuss this sample and their properties in this paper. Wild et al. (2009) discuss the evolutionary importance of this type of galaxy, in terms of their origin as major mergers, and their role in forming the subsequent red sequence. They also note that the density of these galaxies evolves strongly between redshift 0.7 and 0.1.

The luminous galaxies in this sample are in the approximate redshift range 0.2–0.6. Figure 1 shows their distribution in the magnitude/redshift plane, with absolute magnitude contours. While we have a range of redshift and luminosity, these are all the most luminous of the SDSS spectroscopic set. This is their main interest, as they are comparable with luminosites of an active galactic nucleus (AGN). Hoopes et al. (2007) discuss the properties of a generally lower redshift and lower luminosity sample of galaxies.

We note that the SDSS catalog magnitudes used here are the "Petromags," which are generally good measures for compact objects such as these. We have included only sources with formal *GALEX* and *r*-band errors of 0.3 mag or less. We have checked the least and most extended objects (galaxies 1 and 10 in Figure 1 and Table 1) for their different SDSS catalog magnitude values, and find them all to be within ∼0.1, and thus it does not affect our discussions. We also note that the spectra are recorded through fibers that will miss extended flux. The unresolved nature of the galaxies again means that this is not a large effect, and in any case they should form an internally consistent set of spectra.

Table 1 summarizes the galaxy properties and measured quantities. Figure 2 shows several of the SDSS spectra over most of the wavelength range, all shifted to rest wavelengths, for easy comparison. They are stacked for ease of viewing, arranged in order of star formation rate (SFR) from Table 1, and all are scaled to have the same signal at rest wavelength 4000 Å. The mixes of Balmer absorption and emission are evident, as are the different Balmer discontinuities. Notice also the Mg II 2800A doublet, which appears in emission or absorption in three of the galaxies. There is no AGN-type broad emission of Mg II.

The spectra fall into two fairly distinct types—those dominated by star formation and those showing strong post-starburst spectra. Figure 3 shows coadded SDSS spectra of the two types. The spectral region plotted shows the higher Balmer lines and discontinuity, and the [O II] emission. The top plot indicates populations that are mostly post-starburst, although there is still ongoing star formation. The lower plot shows objects still dominated by star formation.

For each spectrum, measurements were made on the Balmer lines and the principal emission lines. Redshifts were derived from both, and in some cases differ from the SDSS cataloged values. The redshifts in Table 1 are those we measured from the spectra. The values for Balmer jump are the ratio of the continuum above and below the Balmer limit, and are accurate to about 10%. The line fluxes and equivalent widths (EWs) were measured directly from the spectra, and converted to absolute fluxes, using the measured redshifts. Line flux ratios among [O II], Hβ, and [O III] were plotted to diagnose the emission-line type of the galaxy. The redshifts of the objects mostly put the Hα and [N II] lines beyond the SDSS spectroscopic wavelength limit, so these lines were available for line ratio diagnostics for only three of the galaxies.

The emission-line ratios indicate that there is no significant AGN component to the spectra: they are all in the LINER or H II galaxy locus of the plots (see, e.g., Terlevich and Melnick 1985). In addition, there were no broad emission features seen in any of their spectra (and we have many SDSS QSO spectra for comparison in the data set). We therefore assume that the full observed fluxes are from the stellar populations alone, plus any intrinsic reddening that may be present.

Star formation rates given in Table 1 are estimated from the [O II] luminosity, using Equation (4) of Kewley et al. (2004). These are subject to uncertainties, as noted, e.g., by Jansen et al. (2001), but as the galaxies are similar in luminosity, we expect them to form an internally consistent set. In the three cases where we have both Hα and [O II], the flux ratios are all very close to

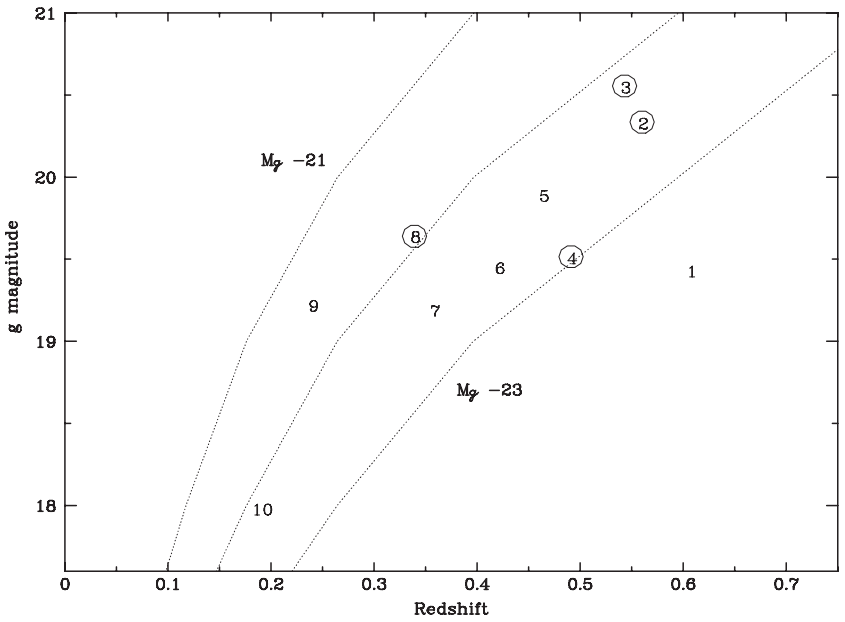

Figure 1. Redshift–magnitude plot for the 10 galaxies. The dotted lines represent loci of absolute *g*-magnitudes, with no *k*-correction, but average local extinction correction. The numbers identify the galaxies from Table 1, and the circled points are those with strong star formation. Except for galaxy 10, the others have post-starburst spectra.

Table 1
Galaxies and Measurements

No.	z	R.A. (deg)	Decl. (deg)	g (mag)	M_g[a]	BD[b]	[O II] (10^{-17} erg^{-1} s^{-1} cm^{-2} A^{-1})	Hβ	[O III]	H8 (*A*)	SFR[c] ($M_\odot$ yr^{-1})	Mg II (km s^{-1})
1	0.603	126.6601	43.09159	19.42	−23.5	1.3	65	26	40	6.5	25	−1170
2	0.556	172.1986	−3.28824	20.32	−22.4	1.3	180	80	330	0	59	NP
3	0.539	46.69901	−8.37817	20.54	−22.3	1.5	150	60	240	0	47	NP
4	0.487	259.0034	27.73754	19.50	−22.9	1.3	500	240	810	0	135	0[d]
5	0.460	319.6005	0.291477	19.88	−22.5	1.6	70	10	40	10	18	NP
6	0.417	21.46781	−8.73612	19.44	−22.5	1.6	260	95	195	7.6	57	−410
7	0.354	217.5169	2.370217	19.18	−22.3	1.4	380	115	360	5.1	69	···
8	0.335	49.39362	−7.97010	19.63	−21.9	1.3	300	135	350	0	52	···
9	0.236	171.3262	−2.45157	19.21	−21.3	1.5	400	120	200	6.9	55	···
10	0.181	124.2052	25.15158	17.97	−21.9	1.0	30	8	52	5.8	4	···

Notes.
[a] No *k*-correction, local extinction corrected.
[b] Ratio of continuum flux above and below the Balmer limit discontinuity.
[c] Star formation rate from [O II].
[d] Emission line.

2. With the exception of the lowest redshift galaxy (10 in the Table), the SFRs are all high, and there is a trend of lower star formation with larger Balmer jump, consistent with decreasing star formation as the stellar population gets older. Again, the lowest redshift galaxy shows no Balmer jump, and appears to be different from the others, although still highly luminous.

We use the Balmer (and He I) emission and absorption line strengths to estimate ages of the starbursts, assuming this is the dominant signature of the spectra. We use the diagnostics outlined by Gonzalez Delgado (1999) and Gonzalez Delgado et al. (1999), and the best-fit ages are about 3 Myr and 10 Myr (with upper limit 50 Myr) for the averaged spectra in Figure 2. The post-starburst mean spectra (Figure 3) are very like the eigenspectrum 1 used by Wild et al. (their Figure 2), so that there is little evidence of what older population may be present. There is a small contribution of Ca II K and the D4000 dip that suggests about 10% presence of eigenspectrum 2, the older population. While the spectra do not have the individual signal-to-noise ratio (S/N) to quantify this more, this puts those galaxies in the post-starburst region of Wild et al.'s diagram (Figure 3). The lowest redshift galaxy has a spectrum that does have strong Ca II and D4000 absorption, Balmer absorption but no Balmer discontinuity, so this galaxy is in a later post-starburst stage, although still very luminous. As this is the only extended object, it is possible that there is a faint younger population in the outer parts of the galaxy, not sampled by the SDSS spectrum.

The Mg II 2800 A doublet is covered in the six highest redshift objects. In three of these, no feature is seen. In one, the line is in emission at the same redshift as the other lines. In the last two, the feature is seen in absorption, and shifted from the galaxy redshift, indicating outflow. This has been noted and discussed by Tremonti et al. (2007) and others, and our outflow velocities implied are 410 and 1170 km s^{-1}. Our galaxy 1 is in their paper, and they measure an outflow velocity of 1231 km s^{-1}, in very close agreement with our value. As they discussed, these galaxies lie just below the distribution of QSOs in the absolute

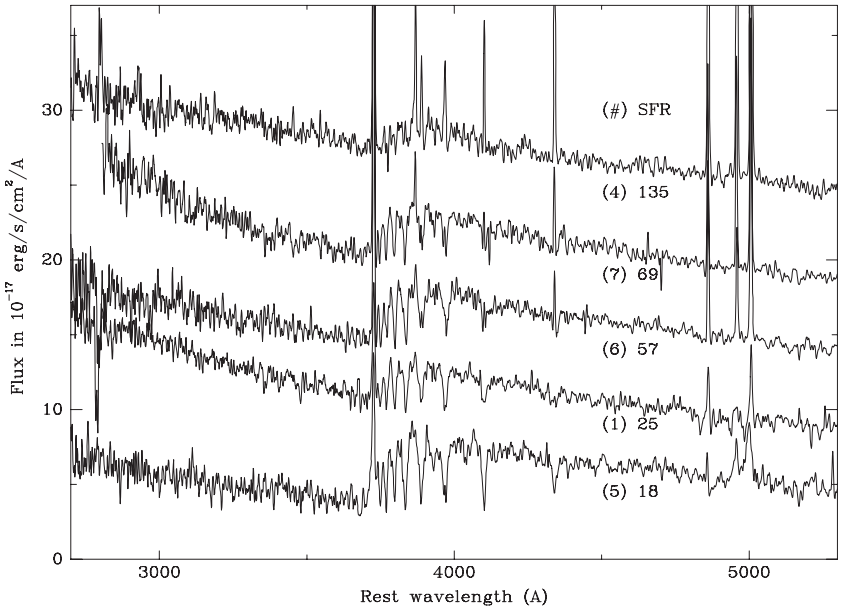

Figure 2. Spectra of five of the sample shifted to rest wavelengths, with flux normalized at rest wavelength 4000 Å. They are separated for easy comparison and arranged in order of star formation derived from the [O II] emission. The numbers in parentheses identify the galaxies in Table 1, and the values given are the SFRs from Table 1, in solar masses per year.

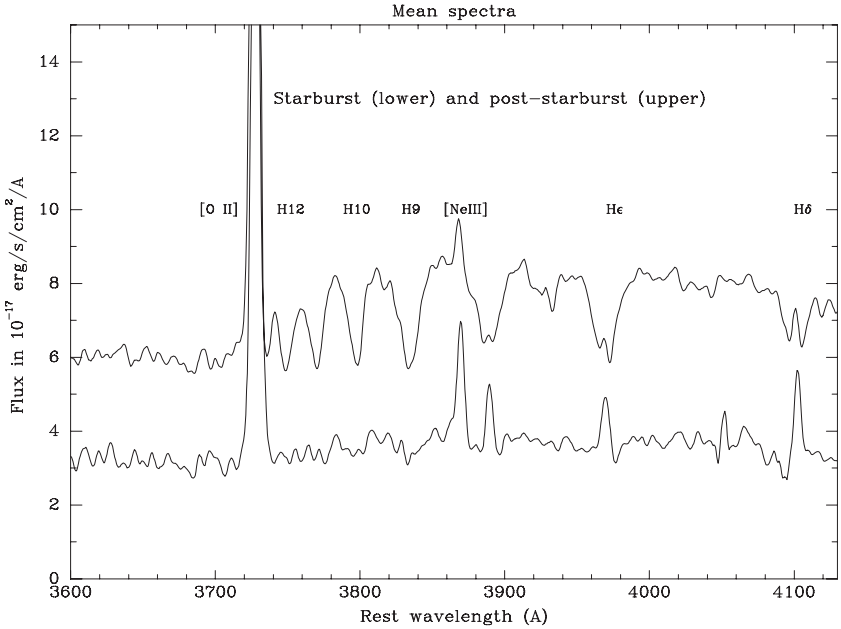

Figure 3. Coadded spectra of two types, shifted to rest wavelengths. Top plot are galaxies 1, 5, 6, 7, 9, and lower plot are galaxies 2, 3, 4, 8 (circled in Figure 1). There is Balmer emission in both plots, but little or no absorption in the lower plot. Note the presence of [O II] and [Ne III] in both. The Balmer EWs in Table 1 are the combined absorption and emission for the Balmer lines.

magnitude versus outflow velocity plot, but we note again that the SDSS spectra show no spectroscopic QSO features.

2. PLOTS AND CORRELATIONS

Figure 4 shows the objects in the two-color plane that was used to define the original QSO sample. The dots are spectroscopically identified QSOs with redshift 1.2–1.5, whose distribution roughly matches the galaxies we are discussing. QSOs of lower and higher redshift have somewhat different distributions within the two-color plane shown. The numbers in Figure 4 are the galaxies as identified in Table 1.

The NUV–*r* and FUV–NUV colors both show correlations with the SFRs in Table 1, and Figure 4 shows "contours" in both colors. FUV–NUV is a measure of the Lyman discontinuity for QSOs of redshift above about 0.64, and otherwise measures the proportion of (unreddened) OB stars in the population, and is thus smaller if there is much star formation. NUV–*r* is also small for active star formation, or the UV continuum of QSOs. The galaxies do not have the extreme FUV–NUV values that higher redshift QSOs have, arising from their Lyman absorptions.

The lines in Figure 4 represent approximate values of SFR (in solar masses per year) from Table 1. The exception to this is galaxy 4, which has by far the largest SFR, at 135 $M_{\odot}$ yr^{-1}.

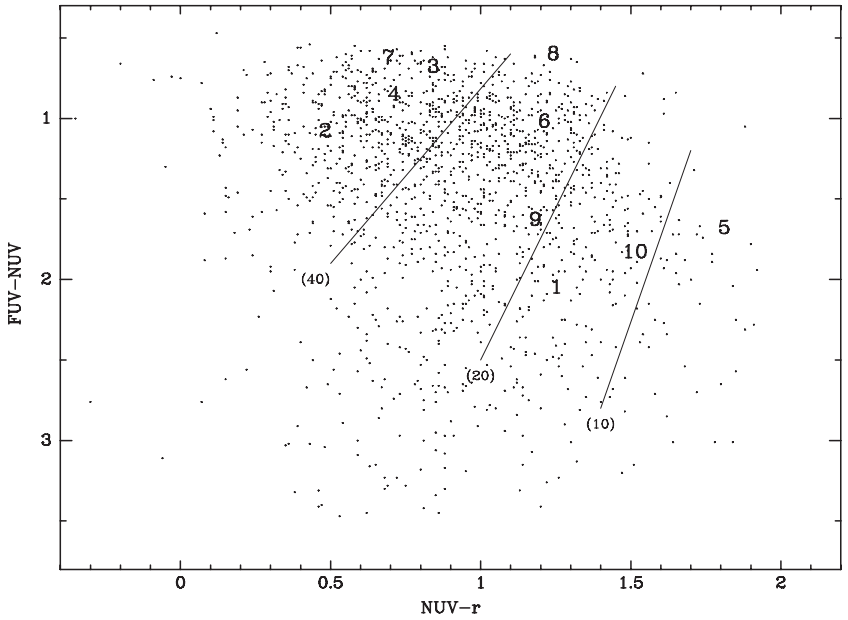

Figure 4. Two-color plane from combined SDSS–*GALEX* photometry. This part of the plane is occupied mostly by QSOs of redshift in the range 0.5–2.0, and the small dots are those in the range 1.2–1.5. The large numbers are the galaxies as numbered in Table 1. The straight lines are rough contours of SFR from Table 1, with values given in brackets in solar masses per year.

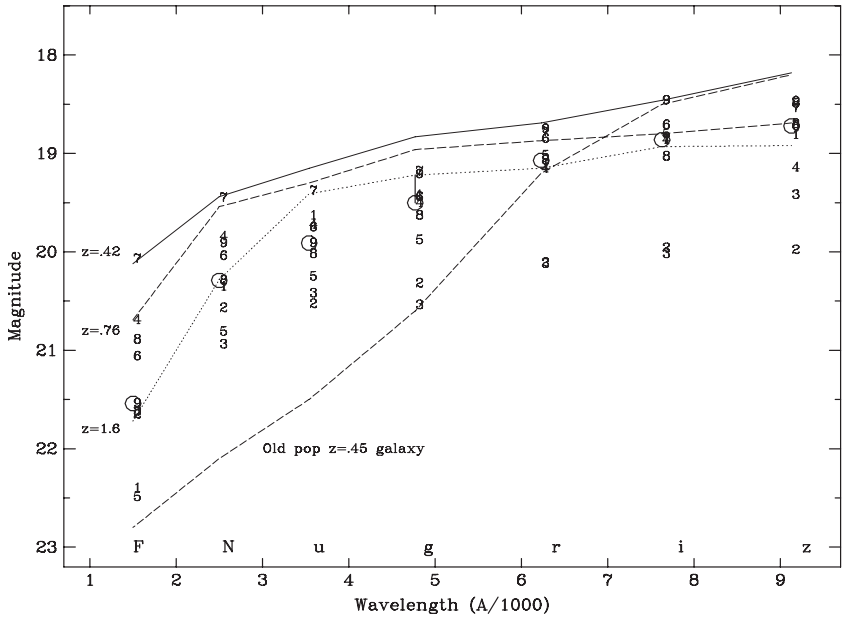

Figure 5. SDSS + *GALEX* magnitudes for the nine galaxies of redshift above 0.2. The one lower redshift galaxy has much brighter visible magnitudes. The numbers are the individual values, and the circles are the medians for the group. The average redshift is 0.44, which puts the Balmer limit absorption in the *g* band. The line running from that median point shows where the continuum would lie without this absorption. The connected points are medians for QSOs at the redshifts indicated, from our sample with the same UV colors. The plot also shows median magnitudes for old-population galaxies in the redshift range 0.4–0.5.

This galaxy has very strong line emission, which could affect its photometric magnitudes. In particular, the NUV channel includes rest wavelength C IV and He II, which would brighten this bandpass, whereas the FUV and *r* bands sample rest wavelengths without strong line emission. A fainter intrinsic NUV magnitude would move the galaxy to the left and up in Figure 4, more consistent with the star formation contours shown. This galaxy is not the most luminous, and we see no indication in the line profiles or ratios that it contains a significant AGN component contributing to the line emission.

Figure 5 shows the *GALEX* and SDSS median magnitudes for these galaxies compared with QSOs in selected redshift bins. The distributions of magnitudes are not Gaussian, and the averages have an overall shallower slope over the full wavelength range. In either case, the galaxy "spectral energy distribution (SED)" is different from QSOs of the same redshift, or other redshift bins. The lower redshift galaxy 10 has a steeper "SED," with brighter visible magnitudes, and is not included. At these redshifts, the *g*-filter bandpass lies in the Balmer limit absorption trough, and a "corrected" median magnitude is indicated by the vertical bar. The magnitudes are all somewhat affected by the emission lines present, in both QSOs and these galaxies.

Figure 5 also shows the median magnitudes for a comparison sample of normal galaxies (i.e., no recent or ongoing star formation), in the redshift range 0.4–0.5. As expected, there

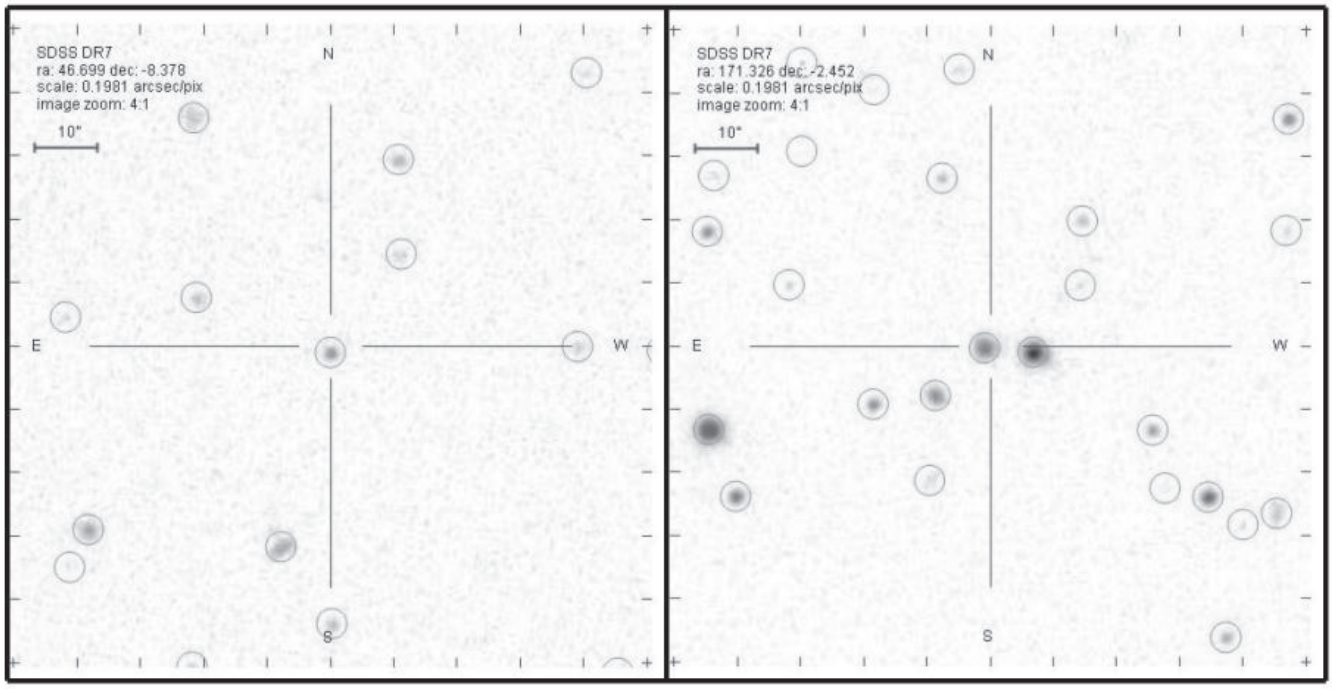

Figure 6. SDSS finding chart images of galaxies 3 (left) and 9 (right) in our list, illustrating a range of density of environments. The circles mark the SDSS catalog objects. We counted only objects easily visible in these images, sometimes omitting empty circles from the SDSS charts, and sometimes adding objects not circled. For instance, there are two empty circles in the right-hand field here. The central galaxies are not resolved, except for galaxy 10.

is increasing flux with wavelength, and the "SED" is quite different.

This comparison sample has some interesting selection effects on its own. The sample of 51 objects was chosen to have SDSS spectra classified as galaxy, in the redshift range 0.4–0.5, but with no color limitations. The redshift range puts all of them in the FUV–NUV range about 0–1.5, but with a wide range of NUV–*r*. Inspection of the spectra showed that 22 are old population galaxies, 12 are lower luminosity QSOs, 5 are starburst galaxies, and 5 are post-starburst. The remaining six are peculiar or too noisy to classify. The NUV–*r* colors get redder very progressively, moving from starburst to QSO to post-starburst, to "normal" galaxies, with the locus of our main sample covering essentially only a few starburst and QSO galaxies. One of the original sample post-starburst galaxies was rediscovered, but the other four are redder in NUV–*r* and have low star formation, as indicated by their [O II] emission. This is consistent with the SFR contours in Figure 4. Their absolute magnitudes are close to −22, so they are not as luminous as the brightest ones in the sample in our table. None of them shows any shifted Mg II absorption.

It is interesting to note that there is a considerable fraction of lower luminosity QSOs that are in the spectra classified as galaxies—about one-fourth in both our original sample and in the comparison sample with larger NUV–*r* values. We also note that some very luminous starburst and post-starburst galaxies lie outside the color selection of our original sample.

Mallery et al. (2007) discuss a sample of galaxies that are similar, but fainter, with combined SDSS and *GALEX* photometry, and Keck spectroscopy. They find galaxies that are somewhat less extreme in UV colors, and on average have lower luminosities and SFRs. They too find that SFRs decline rapidly in the sample from redshifts above to below 0.25.

The post-starburst galaxies can be identified in Table 1 by their Balmer absorption, given by the H8 EW values. This line is chosen rather than Hδ as it will be less contaminated by Balmer emission. The Balmer absorption galaxies have lower SFRs by a factor 2 on average.

We inspected the SDSS images of the 10 galaxy fields, and also a control sample of 6 fields randomly located within a degree of the galaxies. We counted galaxies within a $100'' \times 100''$ box and a $30'' \times 30''$ box around the galaxies and random control sky locations. We also looked for resolved structure of the galaxies themselves. The SDSS image resolution is not ideal for this, and we also found that we did not agree with all the faint "objects" selected by the SDSS photometry pipeline. The results are thus not very conclusive. Galaxy 5 is asymmetrical, and galaxy 10 (the lowest redshift and brightest) is a resolved face-on spiral. The average neighboring galaxy counts in the two box sizes are the same for the galaxy and control fields, at 21 and 1.7. Galaxies 4, 5, and 9 lie in crowded local environments, while 1–3, 6, 10 are in sparsely populated fields. Figure 6 shows the SDSS finder fields for two of the galaxies. Overall, there is no clear indication within the SDSS images that the galaxies are generally in special states or environments.

3. DISCUSSION AND SUMMARY

This group of galaxies comprises all the brightest objects in the spectroscopic sample with FUV–NUV > 0.2 and NUV–$r <$ 2.3, that are not QSOs or local stars. The luminosities overlap the faint side of the QSO distribution, from the same color selection. The QSO's peak is about 1 mag brighter, and there are 361 of them in the same redshift range, in our sample, with SDSS spectra. Thus, the 10 galaxies represent about 3% of the QSO sample at the same redshifts, although the QSO redshifts are skewed to higher values in the range, from our color selection (see Figures 1 and 2 of Bianchi et al. 2009). There are in the sample about 50 less luminous galaxies, all of redshift 0.26 or

less. Our lowest redshift object, chosen for its high luminosity, has a much lower SFR.

Hoopes et al. (2007) discuss a sample of UV-luminous galaxies (UVLGs) from the *GALEX*–SDSS database which are at lower redshifts. In particular, they note the group of compact galaxies, which are similar to Lyman break galaxies (LBGs) at higher redshift. Much of their discussion involves surface brightnesses, but most of our objects are at higher redshift and are not resolved enough to make such estimates. The galaxies in this paper are more luminous than their compact UVLGs and have more extreme FUV–*r* colors, and overall higher SFRs. Our galaxies do not have extreme observed UV flux because their redshift moves Lyman absorption into the FUV band.

It is thus of interest to understand the evolutionary state of these galaxies. It has been suggested that they are massive mergers which have triggered starbursts (Wild et al. 2009). Tremonti et al. (2007) speculate that the outflows are a "fossil galactic wind" triggered when the galaxies were even more luminous, possibly aided by AGN activity, which then quenched the starburst. Amongst our sample, the galaxies dominated by star formation are not more luminous than the others, which therefore does not support this idea. The two most luminous ones of our post-starburst galaxies have Mg II outflow, but they are only marginally more luminous than others which do not. Any outflow absorption seen will depend on what continuum source is seen behind it, so possibly it is localized or orientation dependent. High-resolution imaging of the galaxies should show if tidal events are connected with the star formation.

If we naively measure the star formation episode duration by the Balmer absorption and the instantaneous SFR by the [O II] emission, we see that there is little correlation. Galaxies 6, 7, and 9, appear to be in continued star formation, while 1, 5, and 10 may correspond more to a short starburst that died away. The youngest ones, 2–4 and 8 have all just begun. This is also reflected in the discussion of Basu-Zych et al. (2007).

In summary, we note the following conclusions.

1. These are very luminous galaxies which are within about 10 Myr of a major starburst. In about half, the population is dominated by post-burst stars, and the SFR is lower. A slightly fainter set of such galaxies has redder NUV–*r* colors and lower SFR.
2. While the luminosity overlaps that of QSOs, there are no broad emission lines, and the narrow emission line ratios correspond to H II galaxies.
3. Outflow is seen in two of the galaxies. This is not obviously connected with luminosity, SFR, or age of the starburst.
4. In the FUV, NUV, and *r* band magnitude range used, these galaxies are about 3% of the QSO population at the same redshift. The two-color plane defines rough contours of SFR. The galaxies are not found below redshift 0.2, consistent with cosmic evolution of the population.
5. Based on this spectroscopically confirmed sample, we may expect to find many others in our much larger photometric sample, which we are examining for its QSO population. This should provide more statistics on the overall population of these extreme galaxies, and their evolution.
6. From SDSS imaging, we see no significantly different morphology or environment for these galaxies. Thus, any such evidence must be faint, or unresolved in the SDSS images. If the galaxies are in a post-merger state, then their resolved morphology should clearly reveal that, and add further detail to the scenario. We plan to obtain suitable deep imaging observations.
7. The SDSS spectra classified as galaxy in this redshift and magnitude range contain a significant fraction (∼25%) of QSOs. A number of the SDSS redshifts are incorrect too.

We are grateful to J. Herald and B. Efremova for help in the compilation of the main sample catalogs, from which these objects were extracted.

REFERENCES

Basu-Zych, A. R., et al. 2007, ApJS, 173, 457
Bianchi, L. 2009, Ap& SS, 320, 11
Bianchi, L., Hutchings, J. B., Efremova, B., Herald, J. E., Bressan, A., & Martin, C. 2009, AJ, 137, 3761
Gonzalez Delgado, R. M. 1999, in ASP Conf. Ser. 192, Spectrophotometric Dating of Stars and Galaxies, ed. I. Hubeny, S. Heap, & R. Cornett (San Francisco, CA: ASP), 69
Gonzalez Delgado, R. M., Leitherer, C., & Heckman, T. M. 1999, ApJS, 125, 489
Hoopes, C. G., et al. 2007, ApJS, 173, 441
Jansen, R. A., Franx, M., & Fabricant, D. 2001, ApJ, 551, 825
Kewley, L. J., Geller, M. J., & Jansen, R. A. 2004, AJ, 127, 2002
Mallery, R. P., et al. 2007, ApJS, 173, 471
Terlevich, R., & Melnick, J. 1985, MNRAS, 213, 841
Tremonti, C. A., Moustakas, J., & Diamond-Stanic, A. M. 2007, ApJ, 663, L77
Wild, V., et al. 2009, MNRAS, 395, 144